Dealkanative Main Group Couplings Across the peri-Gap

*Laurence J. Taylor, Michael Bühl, Brian A. Chalmers, Matthew J. Ray, Piotr Wawrzyniak, John C. Walton, David B. Cordes, Alexandra M. Z. Slawin, J. Derek Woollins, Petr Kilian**

Abstract

Here, we highlight the ability of peri-substitution chemistry to promote a series of unique P–P/P–As coupling reactions, which proceed with concomitant C–H bond formation. This dealkanative reactivity represents an interesting and unexpected expansion to the established family of main-group dehydrocoupling reactions. These transformations are exceptionally clean, proceeding essentially quantitatively at relatively low temperatures (70–140 °C), with 100% diastereoselectivity in the products. Mechanistic studies of a representative reaction reveal it to follow second order kinetics, with a remarkably low activation barrier ($\Delta^{\ddagger}H°$ = 57 ± 7 kJ mol^{-1}). The reaction appears to be radical in nature, with the addition of small quantities of radical initiator (azobisisobutyronitrile) increasing the rate dramatically, as well as altering the apparent order of reaction. DFT calculations suggest that the reaction involves dissociation of a phosphorus centred radical (stabilised by the peri-backbone) to the P–P coupled product and a free propyl radical, which carries the chain. This unusual reaction demonstrates the powerful effect that geometric constraints, in this case a rigid scaffold, can have on the reactivity of main group species; an area of research that is gaining increasing prominence in recent years.

1 – Introduction

1.1 – Coupling Reactions and Main Group Catalysis

Coupling reactions, in which two species are linked together with the elimination of a small molecule, have revolutionised many areas of chemical research. In the field of main group chemistry, dehydrocoupling reactions (E–H + H–E' → E–E' + H_2) have provided an alternative to traditional reductive strategies for the formation of E–E bonds. These reactions have been invaluable not only in inorganic synthesis; but also in polymer formation, transfer hydrogenation, and hydrogen storage.[1–3] Meanwhile, cross-coupling reactions have transformed organic synthesis and are widely used in both laboratory and industrial settings.[4–6]

In both fields, main group and organic chemistry, these coupling reactions are typically catalysed by transition metals. This has several drawbacks; many of the metals used are non-abundant and thus expensive, which limits their sustainability and economy. Often, the metals are toxic,[7,8] which leads to problems when these catalysts are used in the synthesis of pharmaceuticals.[9] As such, the replacement of transition metals with cheaper and more readily available main group reagents is a tantalising prospect.

In recent years, there has been a push towards the use of heavier main group elements as catalysts, and a number of reactions which had previously been considered the domain of transition metals have been observed with p-block species.[10] The work of the Radosevich group in this area is particularly exciting, as it demonstrates the profound effect that geometric constraints can have on reactivity.[11–15] By forcing phosphorus into unusual geometries, it is possible to promote atypical reactions such as oxidative addition and reductive elimination (Scheme 1).[14] These redox-active phosphorus compounds can then be built into catalytic cycles, in place of more traditional organometallic catalysts.

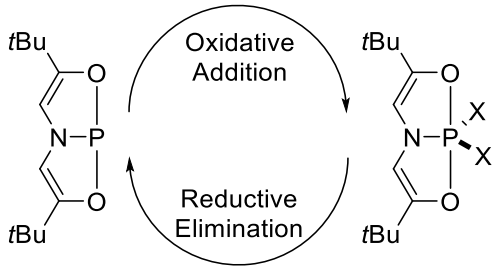

Scheme 1: Oxidative addition and reductive elimination is relatively facile at phosphorus which is geometrically constrained to a T-shaped geometry.[14]

Focusing on dehydrocoupling, a number of main group reagents now exist to effect such transformations, with both stoichiometric[16–20] and catalytic[21–23] examples being known. The majority of these catalytic reagents carry out B–N bond formation,[24–33] with Si–E bond forming reactions (E = C, N, O, S) also being a major area of research.[34–41] While many of these catalysts initially appeared disparate in mechanism, general trends in the reactivity of such species are now being identified as more examples are published.[42] This is expected to lead to the development of better catalysts and increased synthetic utility. It is therefore important that new examples of TM-free dehydrocoupling, and reactions related to dehydrocoupling, continue to be investigated.

1.2 – The use of peri-Substitution to Promote Reactivity

The work of our group has focused on peri-substitution, which is a double substitution in the 1,8 positions of naphthalene, or the 5,6 positions of acenaphthene.[43] The rigid scaffold and enforced proximity this provides is useful in thermodynamically stabilising bonding motifs which are typically unstable at room temperature, such as subvalent or redox metastable species.[43–46] Other groups have used peri-substitution to stabilise free radicals,[47–49] and to generate strong Lewis acids for frustrated Lewis pair chemistry.[50–52]

Lately, we have become interested in using peri-substitution to substantially reduce the *kinetic* barrier to certain reactions, thus eliminating the need for an external catalyst. If successful, we feel that this concept could open an exciting new avenue of research into peri-substitution chemistry. The idea relies on the fact that the two peri-atoms (E) are forced into close proximity, closer than the sum of their van der Waals radii. This introduces significant strain into the system, which is thermodynamically unfavourable.[53] If possible, the system will seek to relieve that strain, and one way to achieve that is to undergo a coupling reaction. By forming a direct E–E bond, or by bonding via a bridging atom, the peri-backbone can achieve a far more relaxed geometry. In such a reaction, the peri-scaffold emulates the role of a catalyst by fixing the two reacting groups in place (reducing conformational entropy), destabilising

the starting material relative to the transition state, and potentially by stabilising the transition state. Thus, the overall kinetic energy barrier is reduced, allowing the reactions to proceed at a reduced temperature. Scheme 2 illustrates these effects on an example P–P coupling reaction.

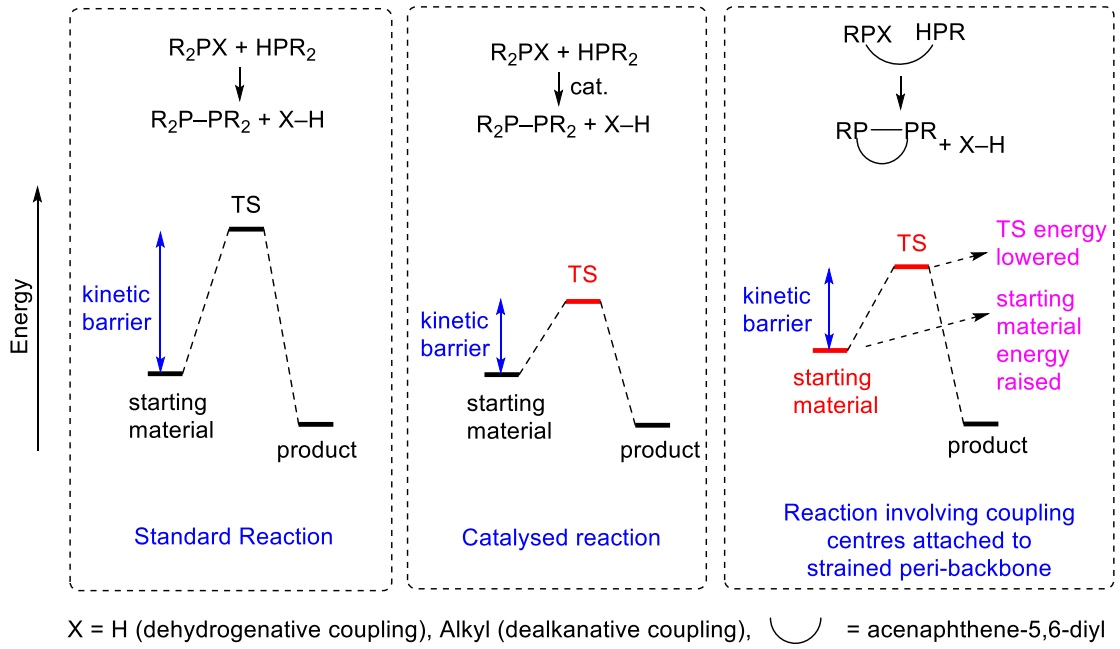

Scheme 2 General scheme highlighting the differences in the kinetic barriers of selected phosphine-phosphine couplings. Energy profiles for the reaction in the presence and absence of a catalyst, as well as for the strained peri-system, are shown. Altered energy levels (in the catalysed and peri-substituted systems) are highlighted in red.

This concept has already been demonstrated in our recent work on peri-substituted phosphine-borane adducts. These molecules were found to undergo a spontaneous P–B dehydrocoupling reaction to afford P–B–P bridged species (Scheme 3, top).[54] This reaction occurred at room temperature and in the absence of a catalyst, something which had never been observed previously.[55,56]

In this paper, we extend this "enforced proximity coupling" concept to a series of highly unusual dehydrocoupling and dealkacoupling reactions, in which a direct E–E bond (E = P, As) is formed with concomitant elimination of either dihydrogen or a C–H coupled product, propane (Scheme 3, bottom). We also present a detailed mechanistic investigation of a representative dealkacoupling reaction, which reveals the transformation to be rather remarkable, involving the spontaneous formation of radicals and subsequent selective propagation under surprisingly mild conditions.

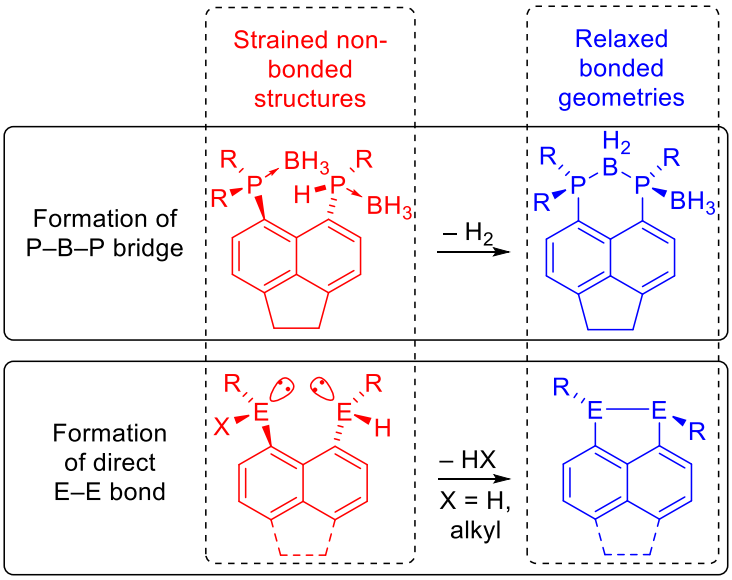

Scheme 3 Relaxation of the strained peri-geometry via P–B[54] or E–E coupling (E = P, As; as reported herein) with concurrent formation of either H_2 or an alkane.

2 – Results and Discussion

2.1 – Thermally Induced Dehydrocoupling

To date, only two examples of direct E–E dehydrocoupling on a peri-substituted scaffold (Scheme 3, bottom) have been reported. In 2004, Schmidbaur synthesised the primary bis(phosphine) **1** by reduction of Nap(PCl_2)$_2$ with $LiAlH_4$ (Nap = naphthalene-1,8-diyl), and observed diphosphane **2** as a minor by-product (Scheme 4). This compound was proposed to form via a dehydrogenative P–P coupling reaction from **1**. However, this transformation was not studied in detail, and compound **2** was characterised in the mixture with **1** by mass spectrometry and $^{31}P\{^1H\}$ NMR only.[57]

The transformation of bis(phosphine) **1** to diphosphane **2** has been reinvestigated by us and, in the process, a new route to **1** and **2** *via* the phosphonium-phosphoride Nap(P_2Cl_6) has been developed (Scheme 4).[58] In our hands, both reductions (of Nap(PCl_2)$_2$ or Nap(P_2Cl_6)) afforded mixtures of **1** and **2** in variable ratios. Heating a mixture of **1** and **2** (with an initial ratio of 1:4) to 140° C in an inert solvent (xylenes) for 5 days gave complete, clean conversion to compound **2** (Scheme 4) as judged by $^{31}P\{^1H\}$ NMR. This confirmed that catalyst-free dehydrocoupling of **1** is possible at moderate temperatures, and allowed pure **2** to be isolated and fully characterised, including by single crystal X-ray diffraction (Figure 1).[59]

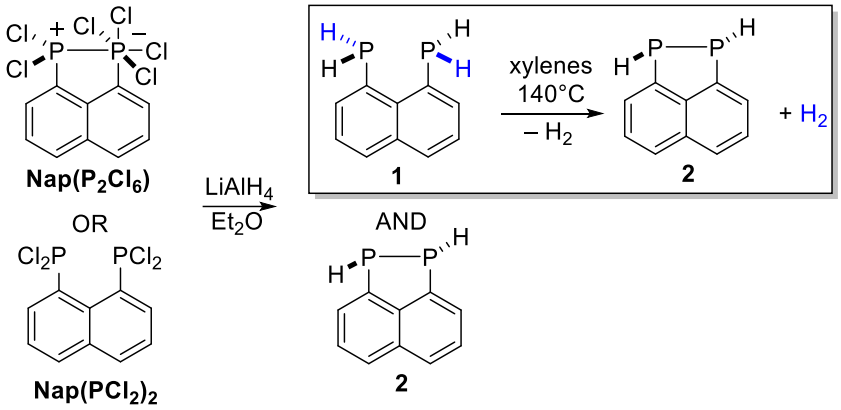

Scheme 4: Synthetic transformations leading to $Nap(PH)_2$ (**2**). Complete conversion of **1** to **2**, from an initial mixture of **1** and **2** containing approximately 80% **2**, took 5 days at 140 °C. The dehydrocoupling step is highlighted in the frame.

To put this reactivity into context, we highlight here the *catalytic* dehydrocoupling of a closely related bis(phosphine), *o*-$C_6H_4(PH_2)_2$. The mildest conditions for this substrate (as reported by Stephan) were 75 °C for 48 hours in the presence of 5 mol% [CpTi(NP*t*Bu)$(CH_2)_2$], which gave the dimer $[C_6H_4P(PH)]_2$ in 75% isolated yield.[60] Waterman carried out the same transformation using a zirconium catalyst, with full conversion requiring temperatures of 100 °C for 4–6 weeks.[61] We presume the related uncatalysed reaction would require harsher conditions, presumably significantly harsher than those used in our uncatalysed transformation of **1** to **2**. In short, the clean thermal dehydrocoupling of bis(phosphine) **1** is unusual, as it is comparable (in terms of rate and reaction temperatures) to the transition metal catalysed dehydrocoupling of electronically similar substrates.

The only other example of a direct E–E dehydrocoupling arising from peri-substitution is the synthesis of the stable arsanylidene-σ^4-phosphorane **4**, recently published by our group.[45] This was obtained by dehydrogenative coupling of the primary arsine **3** (Scheme 5, top). This reaction is very unusual, representing both a rare 1,1-hydrogen elimination and an example of dehydrocoupling being employed in the synthesis of a low-valent main group species.

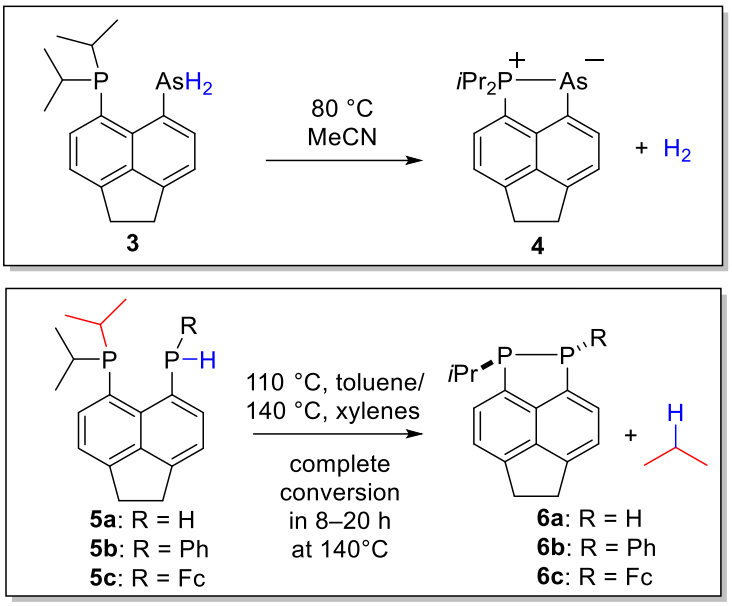

Scheme 5: Contrasting outcomes of the dehydrogenative P–As coupling to afford arsanylidene-σ⁴-phosphorane **4** (top) and of the dealkanative P–P couplings of bis(phosphines) **5a–c** (bottom).

2.2 – Thermally Induced Dealkacoupling

2.2.1 – Phosphorus-Phosphorus Dealkacoupling

As the primary arsine **3** (Scheme 5, top) had displayed such interesting reactivity on heating, the thermal decomposition of the phosphorus congener (the primary phosphine **5a**) was investigated, with unexpected results. On refluxing **5a** in toluene for 3 days (or xylenes for 8 h), clean conversion to the diphosphane **6a** was observed (Scheme 5, bottom). In this reaction, **5a** undergoes P–P coupling, with concomitant C–H bond formation to evolve propane gas. The evolution of propane was confirmed by trapping the gaseous byproducts and subsequent analysis by ^{1}H NMR (see supporting information (SI), section 6.1). No evidence of propene or hydrogen formation was observed in this experiment. The reaction proceeded essentially quantitatively, with very minor amounts of other phosphorus compounds being co-formed (< 2% as judged by ^{31}P NMR).

As an extension to this, two other secondary phosphines (**5b–c**) were synthesised via previously published procedures[62,63] and heated in toluene or xylenes. These compounds also underwent propane elimination to yield the novel diphosphanes **6b–c** in quantitative yield (Scheme 5, bottom). These reactions are exceptionally clean, with no phosphorus containing byproducts being observed. X-ray crystallography demonstrated that these diphosphanes form exclusively as the trans isomers (Figure 1). Both structures show a decrease in strain compared to the parent bis(phosphines) **5b–c**, with reduced P···P distances (**6b**: 2.232(2) Å, **6c**: 2.220(2) Å; c.f. **5b**: 3.028(1) Å, **5c**: 3.050(2) Å),[62] splay angles (**6b**: −7.8(13)°, **6c**: −8.2(4)°; c.f. **5b**: +11.0(10)°, **5c**: +12.2(9)°)[62] and almost no out-of-plane displacement of the peri-atoms (see Table 1).

Whilst approximately the same rate of elimination was observed for both **5a** and **5b**, the rate of propane elimination for the ferrocenyl compound (**5c**) was substantially slower. Complete conversion was achieved after 20 hours of reflux in xylenes, or 15 days in toluene (c.f. 3 days in toluene for **5a**).

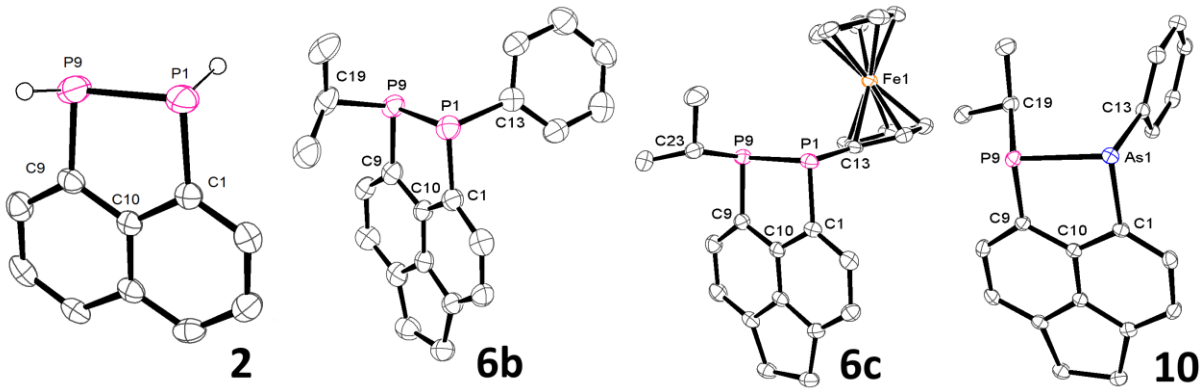

Figure 1 Structures of **2**, **6b**, **6c** and **10** in the solid state. Carbon-bound hydrogen atoms and second molecule in asymmetric unit (**6b**, **10**) omitted for clarity. The phosphorus-bound hydrogens of compound **2** are disordered over two positions, but are believed to be trans to one another. For clarity, only one pair of H atoms is shown.

This C–H bond forming reaction is unexpected and rather intriguing. Almost all work on E–E couplings thus far has involved the evolution of hydrogen,[1–3] whilst related main group dealkanative reactivity (E–H + E–R → E–E + R–H; E = main group element, R = alkyl) is mostly limited to systems involving highly energised and polar M–C bonds. Examples of this include the reaction of metal alkyls (M = Li, Al, Mg, Zn) with protic substrates (for example Et_3Al + E–H → Et_2Al–E + EtH). In contrast to M–C bonds, P–C bonds are rather non-polar (χ(P) = 2.19; χ(C) = 2.55 on the Pauling scale)[64] and are considered to be one of the most stable bonds in chemistry.[65] Alkane elimination also occurs in the production of semiconductor films by metalorganic vapour phase epitaxy (MOVPE; i.e. $InMe_3$ + AsH_3 → 3 CH_4 + InAs).[66] However, such reactions proceed at very high temperatures (600–700 °C), far beyond those employed in this reaction.[67]

Somewhat more distant from pnictogen chemistry; an intriguing example of ambient temperature demethanative Ge–Ge coupling [n($HGeMe_3$) → $H(GeMe_2)_nMe$ + (n−1)CH_4] was reported by Berry in 1996.[68,69] More recently, the group of Hill has reported a catalytic B–N coupling reaction proceeding with concurrent formation of a Si–H bond (elimination of Me_2PhSiH, a "desilacoupling" reaction).[70] However, although superficially similar, both of these reactions appear mechanistically distinct from this propane elimination. The demethanative coupling requires a ruthenium metal catalyst, while the "desilacoupling" is mediated by strongly basic group 2 metal reagents.

2.2.2 – Phosphorus-Arsenic Dealkacoupling

As an initial expansion of this work, we decided to move down group 15 to the heavier pnictogens. These elements form weaker E–H and E–C bonds and, as such, might be expected to eliminate more readily than the P/P system. To this end, an arsenic analogue of the bis(phosphine) **5b** (**9**) was synthesised, to see if it underwent propane elimination at an increased rate.[71] To synthesise **9**, Acenap(P*i*Pr_2)(Br) (Acenap = acenaphthene-5,6-diyl) was treated with *n*BuLi and then reacted with 1 equivalent of $PhAsCl_2$.

This afforded a mixture of compounds **7** and **8**,[72] which were then reduced with $LiAlH_4$ to obtain the target compound (Scheme 6).

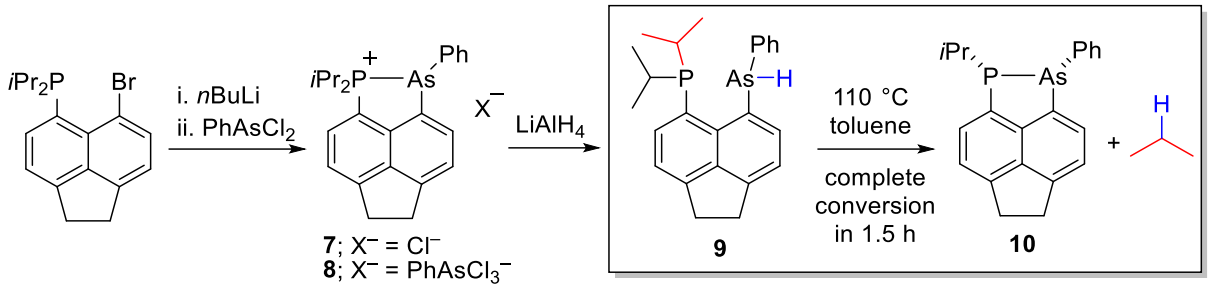

Scheme 6: Synthesis of arsenic compounds **7**, **8**, and **9,** followed by propane elimination to give **10** (highlighted in the frame).

Compound **9** was subjected to heating and, as predicted, eliminated propane to give the P–As bonded compound **10** at a far faster rate than its phosphorus congener. Complete clean conversion to **10** was achieved after 1.5 h of reflux in toluene, with **5b** requiring 3 days under the same conditions. Intriguingly, the crystal structure of **10** (Figure 1) demonstrated that compound **9** eliminated propane to give exclusively the cis product, whereas bis(phosphines) **5b–c** gave exclusively the trans isomer (Figure 1). In the crystal structure, compound **10** (as with the related diphosphanes **6b–c**) is relatively unstrained with a slightly negative splay angle and minimal out-of-plane displacements (Table 1). The P–As bond length (2.387(1) Å) is typical of a standard P–As single bond.[73]

To the best of our knowledge, the mild thermal elimination of an alkane from P–H/As–H and P–C functionalities is without precedent in the literature. Most notably, this reactivity involves the cleavage of a strong, non-polar P–C bond without the need for bond activation via the addition of a catalyst. We have undertaken a detailed mechanistic investigation into this reaction, as detailed below.

Table 1: Selected bond lengths (Å), out-of-plane displacements (Å) and angles (°) for **2**, **5b**, **6b**, **6c** and **10**.

Compound	**2**	**5b**	**6b**[a]	**6c**	**10**[a]
E1···P9[b]	2.199(1)	3.028(1)	2.232(2) [2.231(2)]	2.220(2)	2.3867(8) [2.3870(9)]
Out of plane displacement (E1)[b]	0.024	0.351	0.013 [0.032]	0.247	0.008 [0.173]
Out of plane displacement (P9)	0.027	0.323	0.026 [0.104]	0.089	0.164 [0.111]
Splay angle[c]	−7.8(6)	+11.0(10)	−7.8(13) [−8.1(13)]	−8.2(4)	−4.2(6) [−4.5(6)]

a) Measurements for second molecule in asymmetric unit shown in square brackets; b) E = P, As; c) Splay angle = sum of the three bay-region angles – 360°. Example (for compound **2**): P9–C9–C10 + C9–C10–C1 + C10–C1–P1 – 360°.

2.3 – Mechanistic Studies of Propane Elimination

2.3.1 – Eyring Analysis and Solvent Effects

We focused on the conversion of **5b** to **6b** (Scheme 5, bottom), as this reaction was considered representative, and the synthesis and purification of **5b** could be conducted on a relatively large scale with little difficulty. The progress of the reaction was monitored by taking aliquots of the reaction mixture at pre-determined time points, and analysing them by quantitative $^{31}P\{^{1}H\}$ NMR spectroscopy. Full experimental details for these measurements are given in sections 6.2 and 6.3 of the SI.

The reaction of **5b** to **6b** in xylenes proceeded cleanly, with no observable intermediates or by-products (Figure 2, A). The reaction was found to be second order with respect to **5b**, with a rate constant of 57 ± 2 M^{-1} h^{-1} (T_{rxn} = 131 ± 1 °C; Figure 2, B).[74] Changing to a more polar reaction solvent (benzonitrile; Figure 2, B) did not change the order of reaction, but resulted in a substantial drop in rate to 7.4 M^{-1} h^{-1} (T_{rxn} = 128 ± 1 °C). This suggests that the rate controlling step does not involve a significant build-up of charge, and makes an ionic mechanism unlikely.[75] Such a substantial drop in rate constant on switching to a more polar solvent is unusual, but may be due to stronger solute-solvent interactions in benzonitrile compared to xylenes, which could hinder the approach to the transition state.

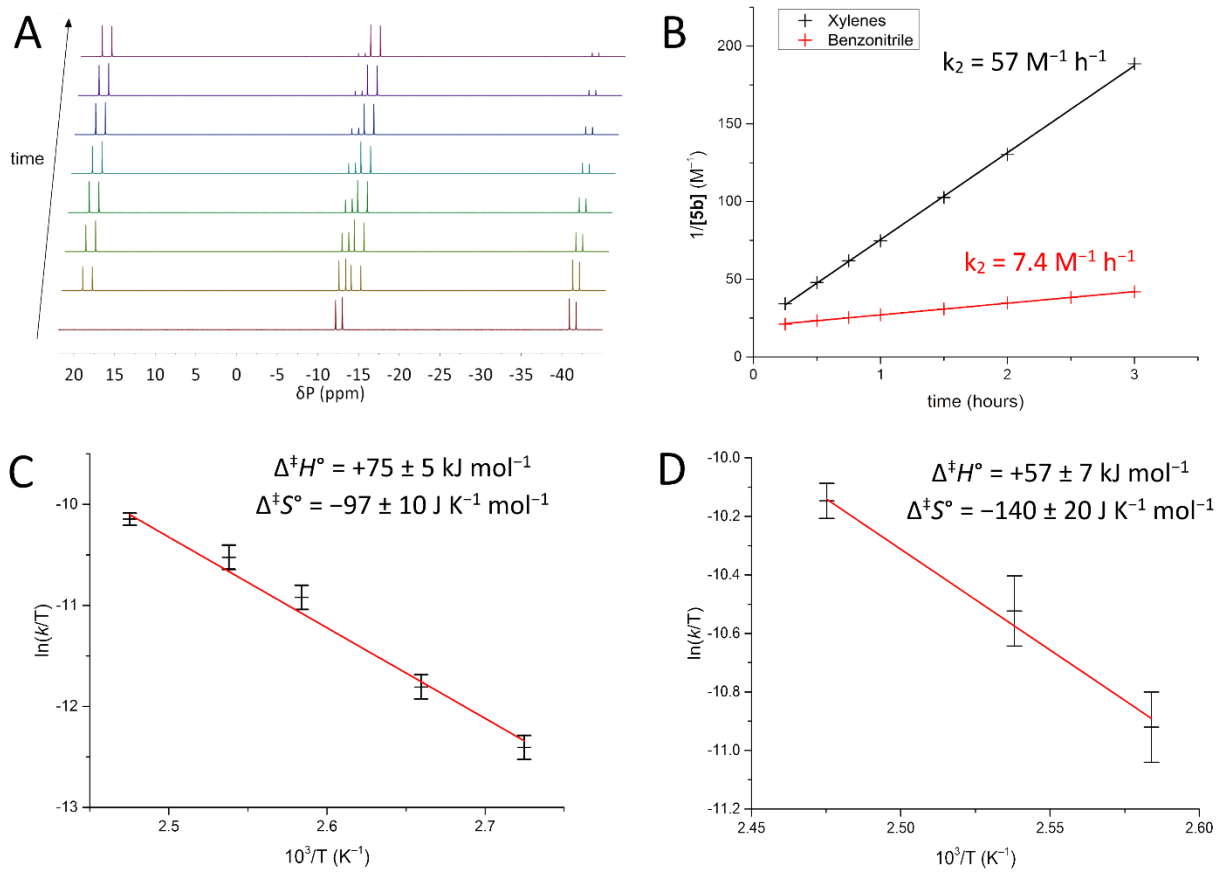

Figure 2: Mechanistic data for dealkanative coupling of **5b** to **6b**. (A) Time-stacked quantitative $^{31}P\{^1H\}$ NMR spectra showing the consumption of **5b** and formation of **6b**. (B) Second order rate plot (inverse concentration vs. time) for reactions in xylenes (T_{rxn} = 132 ± 1 °C) and benzonitrile (T_{rxn} = 128 ± 1 °C). (C) Eyring plot for data collected over the temperature range 94–132 °C in xylenes. (D) Eyring plot for data collected over the temperature range 114–131 °C in xylenes. Error bars set to 3σ for T_{rxn} = 131 °C (based on 3 independent measurements at this temperature) and twice this value for all other data points (which were measured once only).

Second order rate constants were obtained for the reaction in xylenes over a temperature range of 94–131 °C. While reactions in the range 114–131 °C gave data that clearly fit second order kinetics, the measurements at lower temperatures were less clear. When data obtained in the range 94–103 °C were plotted, a very slight curvature was observed in the second order rate plots (see SI, section 6.4). This could be due to systematic error, or could indicate a change in mechanism. Plotting an Eyring graph over the full temperature range affords activation parameters of $\Delta^{\ddagger}H°$ = +75 ± 5 kJ mol^{-1} and $\Delta^{\ddagger}S°$ = −97 ± 10 J K^{-1} mol^{-1} (Figure 2, C). However, a better linear fit is obtained with data in the range 114–131 °C only (Figure 2, D). Because of the uncertainty associated with the rate constants measured at lower temperatures, we feel it is prudent to exclude these data points from the Eyring plot. This affords activation parameters of $\Delta^{\ddagger}H°$ = +57 ± 7 kJ mol^{-1} and $\Delta^{\ddagger}S°$ = −140 ± 20 J K^{-1} mol^{-1}.

This activation enthalpy is remarkably low, much lower than the bond dissociation energies of either of the bonds being cleaved in this reaction. This suggests the mechanism is in some way concerted, with simultaneous bond formation and bond cleavage. The negative entropy of activation could indicate some degree of ordering in the transition state, perhaps the association of two molecules.

2.3.2 – Kinetic Isotope Effect (KIE)

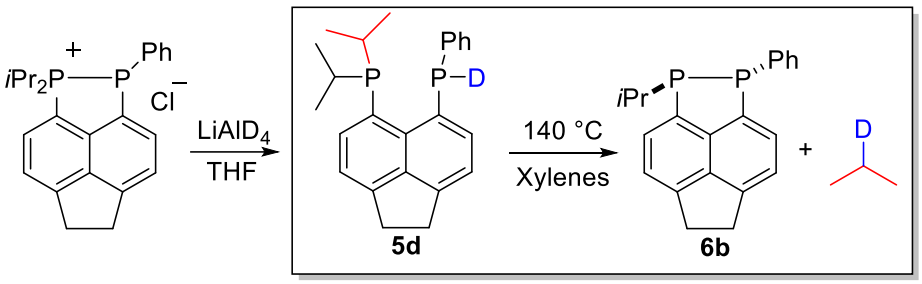

Scheme 7: Synthesis of deuterated compound **5d**, and thermal elimination of propane-2-*d* to afford **6b**.

The deuterated analogue of **5b**, compound **5d**, was synthesised by reduction of the phosphino-phosphonium salt [Acenap(P*i*Pr$_2$)(PPh)][Cl][62] with lithium aluminium deuteride (Scheme 7). Compound **5d**, somewhat surprisingly, proved difficult to handle due to the labile nature of the P–D bond. Exposure to the slightest trace of moisture resulted in loss of the deuterium label and formation of the unlabelled **5b**. Furthermore, it was found that **5b** would not convert back to **5d** on stirring with excess D_2O, even in the presence of a base (LiOD). While this result was unexpected, similar isotopic discrimination against deuterium by phosphorus has been previously observed by Zhang and Mao.[76]

Because of this instability, it was not possible to purify **5d** by recrystallisation from acetonitrile, as this resulted in significant loss of label (even under strictly anhydrous conditions). Also, attempting to monitor the reaction rate of **5d** by the same method employed above was not successful, as taking aliquots always led to some conversion of **5d** to **5b** and subsequent distortion of the measurements.

To circumvent this, two stock solutions of **5d** and **5b** (of similar concentration in xylenes) were prepared in flame-sealed NMR tubes under argon. These were then heated in the same preheated oil bath (T_{bath} = 140 °C) for the same amount of time (15 minutes), and then analysed by quantitative $^{31}P\{^1H\}$ NMR spectroscopy (see SI, section 6.5). This gave an approximate value for k_H/k_D of 5, based on the amount of starting material consumed. While this method does not afford a high degree of accuracy, the difference in rates is substantial, and unlikely to be solely due to error. Because of this large kinetic isotope effect, we conclude that cleavage of the P–D/P–H bond is likely involved in the rate controlling step of this reaction.

A second sealed NMR sample of **5d** was prepared and heated for 3 days at 140 °C, until almost all starting material had been consumed. This sample was then analysed by $^2H\{^1H\}$ and ^2H NMR spectroscopy, which clearly showed the presence of the expected elimination product, propane-2-*d* (Scheme 7).[77] No other deuterated compounds were observed, indicating no isotope scrambling had occurred during the reaction in the sealed system.

2.3.3 – The Effect of Radical Scavenger and Initiator

The thermal reaction of **5b** was also carried out in the presence of an excess (≈ 10 equivalents) of the radical scavenger 1,4-cyclohexadiene.[78–80] This had a rather dramatic effect, resulting in no propane elimination when the reaction was run for over an hour in xylenes (T_{rxn} = 128 ± 1 °C).[81] During this time,

no phosphorus containing compounds (other than the starting material) were observed by $^{31}P\{^{1}H\}$ NMR spectroscopy.

The reaction was then carried out in the presence of the radical initiator azobisisobutyronitrile (AIBN). With the addition of 10 mol% AIBN at 72 °C in benzene, a solution of **5b** underwent complete conversion to **6b** within 15 minutes; a huge increase in reaction rate. The reaction was still exceptionally clean, with no other significant peaks observed in the $^{31}P\{^{1}H\}$ NMR. With 0.5 mol% AIBN, the reaction was still accelerated, but could be monitored by the method employed previously. The reaction was now found to be pseudo-first order in **5b** (k_{obs} = 0.055 min^{-1}, T_{rxn} = 72 ± 1 °C, Figure 3).

This result is interesting from a synthetic perspective, as well as a mechanistic one. The addition of a very small amount of radical initiator has allowed the reaction to occur faster, under milder conditions, with no loss of stereoselectivity or increase in side-products. It is likely that other, similar reactions will also be enhanced, and this could be helpful in designing synthetically useful transformations based on this reactivity. Given the substantial changes observed on addition of both a radical initiator and radical scavenger, it seems highly likely that this reaction occurs via a radical mechanism.

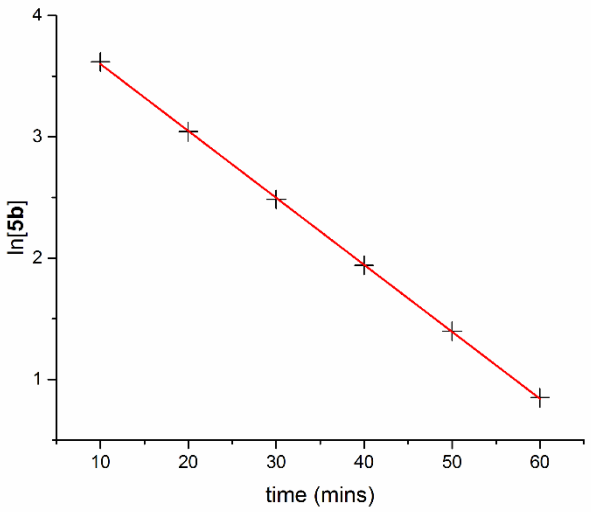

Figure 3: 1st order rate plot for propane elimination from **5b** in the presence of 0.5 mol% radical initiator AIBN (T_{rxn} = 72 ± 1 °C, benzene).

Electron Paramagnetic Resonance (EPR) spectroscopy was employed to help identify any transient radical intermediates. Radicals were generated in situ by either raising the temperature (to a maximum of 370 K), or irradiating with UV light in the presence of an initiator (di-*tert*-butyl peroxide, DTBP) at 250–300 K (see SI, section 2). However, no appreciable signal was observed in either experiment. This is most likely due to the radicals being too short lived, or giving signals that are too broad to resolve.

To summarise the experimental observations, we can conclude that this reaction likely proceeds by a radical chain mechanism, and that this mechanism (in the absence of a radical initiator) must afford a rate equation that is overall second order in **5b**. The rate controlling step likely involves cleavage of the P–H bond due to the significant KIE observed, and deuterium labelling shows that the phosphorus-bound hydrogen is selectively transferred to C-2 of propane. The experimentally determined activation

parameters will be dependent on every step in the radical chain, and therefore are difficult to interpret directly, but the low value of $\Delta^{\ddagger}H°$ suggests that high enthalpy transition states are unlikely to be involved.

2.4 – Mechanistic Discussion

2.4.1 – Mechanism with a Radical Initiator

We begin by considering the reaction in the presence of the radical initiator AIBN. Under these conditions, the radical chain is simplified, as the initiation step (dissociation of AIBN into two 2-cyanopropyl radicals, R·) is known. After this, the reaction likely begins with hydrogen abstraction from **5b** by R·, to afford a new phosphorus centred radical, (**5b**-H)· (Scheme 8, Reaction 1). The reaction has a modest activation barrier ($\Delta^{\ddagger}G°$ = +57.5 kJ mol^{-1} at 345 K), which is achievable under the reaction conditions. DFT calculations reveal that (**5b**-H)· can undergo P–C bond cleavage, affording **6b** and the propyl radical, Pr· (Scheme 8, Reaction 2). This is an equilibrium process ($\Delta_r G°$ ca. +11.5 kJ mol^{-1} at 345 K)[82] with a surmountable energy barrier ($\Delta^{\ddagger}H°$ = +63.1 kJ mol^{-1}). It should be noted that elimination to form the trans-diphosphane is more favourable than formation of the cis-isomer ($\Delta\Delta^{\ddagger}G°$ = 10.7 kJ mol^{-1} at 345 K), which correlates with the observed stereoselectivity.

Once formed, the propyl radical (Pr·) can abstract a hydrogen atom from another molecule of **5b**, affording (**5b**-H)· and propane (PrH). This step has a very strong driving force ($\Delta_r G°$ ca. −120.9 kJ mol^{-1} at 345 K), and is essentially diffusion controlled with no enthalpic barrier (Scheme 8, Reaction 3).

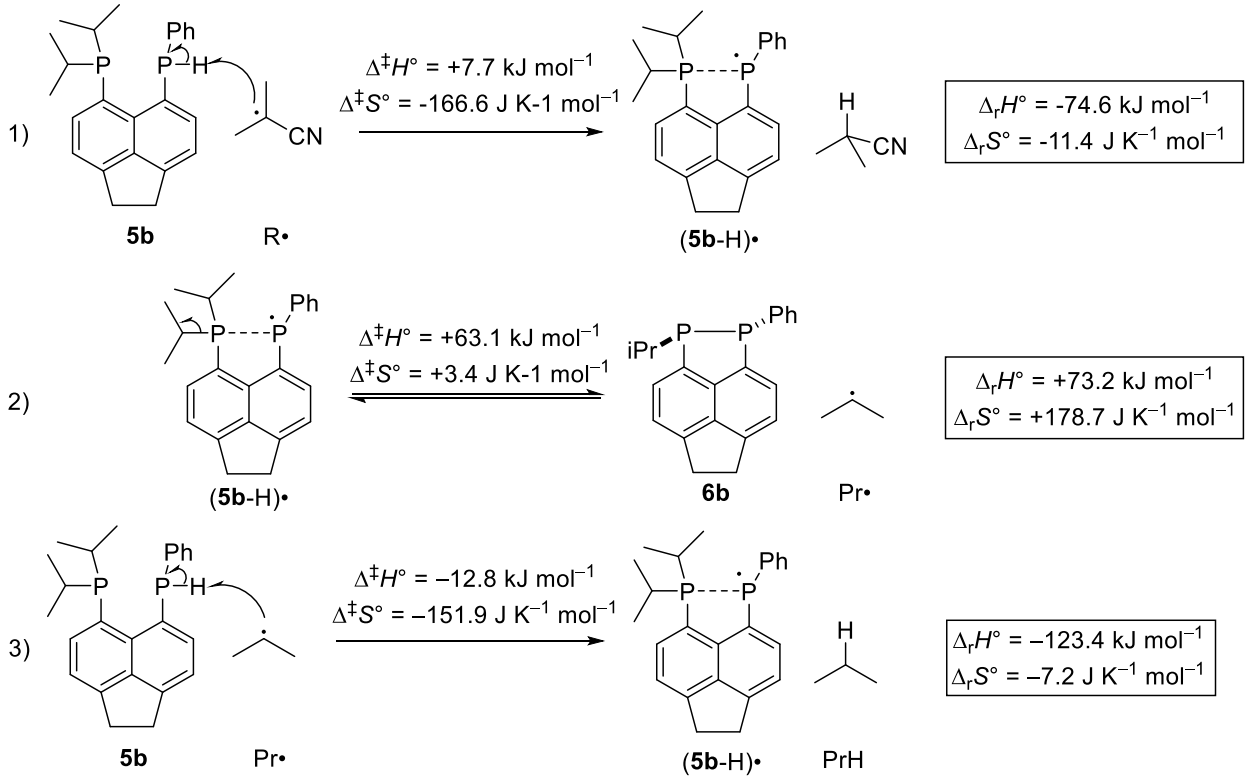

Scheme 8: Proposed radical chain for propane elimination in the presence of AIBN, with computed activation parameters and thermodynamic driving forces shown.

The radical chain shown in Scheme 8 is analogous, kinetically speaking, to that found in a typical free-radical polymerisation reaction carried out in the presence of a radical initiator.[83] We can therefore write the expected rate equation using a known result from polymer chemistry:[84]

$$rate = k[\mathbf{5b}][AIBN]^{\frac{1}{2}} \quad (1)$$

Thus, this mechanism predicts a reaction that is first order in **5b**, as observed experimentally (Figure 3). Running the reaction with a two-fold increase in AIBN concentration (1.0 mol%) resulted in the observed rate constant increasing by a factor of 1.5 (≈ $\sqrt{2}$). This is taken as further support for the mechanism shown in Scheme 8.

The structure of the proposed radical (**5b**-H)· was probed in silico, to determine if it is a plausible intermediate for the reaction. Formation of the radical results in a partial relaxation of strain (with respect to **5b**), as seen in the reduction of the peri-distance (Figure 4). There is an increase in the calculated Wiberg bond index (WBI = 0.18 in B; c.f. 0.01 in **5b**), consistent with a weakly bonding interaction between the two P atoms. The radical also shows significant spin delocalisation across both phosphorus atoms (calculated spin densities; P1 = 0.80, P9 = 0.11).[85]

From this, we conclude that (**5b**-H)· is somewhat stabilised by the peri-backbone. The rigid backbone will promote and stabilise the formation of a weakly bonding interaction between the two phosphorus atoms, in which lone pair density from atom P9 is partially transferred to the electron deficient radical centre (P1). In fact, peri-substitution has previously been used to stabilise several radical species for this reason, including boryl[47] and chalcogen[48,49] radicals. This additional stabilisation may be crucial in allowing this reaction to proceed (especially in the absence of AIBN) as one would not normally expect homolytic cleavage of P–H or P–C bonds to occur under such mild conditions. Furthermore, this stabilisation supports the notion that (**5b**-H)· is a plausible (albeit short lived) intermediate of the reaction.

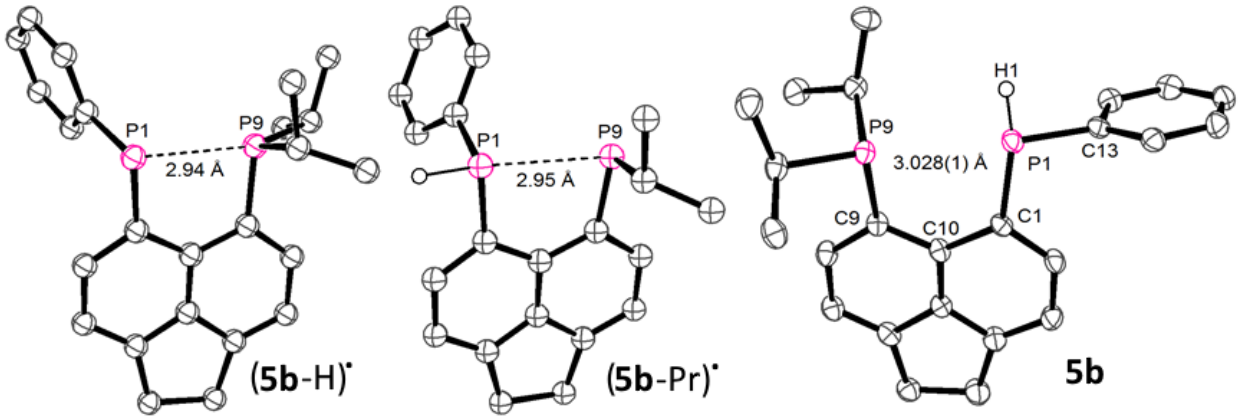

Figure 4: Optimised geometries (B3LYP level) for proposed radical species (**5b**-H)· (left) and (**5b**-Pr)· (middle), with the solid state structure (from single crystal diffraction) of the starting material (**5b**) shown on the right for comparison. Carbon bound hydrogen atoms are omitted for clarity.

2.4.2 – Mechanism without a Radical Initiator

Given that the propagation steps proposed above (Scheme 8, Reactions 2 and 3) account for the observed products and are energetically accessible, it seems reasonable that the same propagation steps operate in the absence of an initiator. It is interesting to note that the computed enthalpic barrier for

dissociation of radical (**5b**-H)· ($\Delta^{\ddagger}H°$ = +63.1 kJ mol^{-1}, Equation 2 in Scheme 8), and the entropic barrier for hydrogen abstraction by Pr· ($\Delta^{\ddagger}S°$ = −151.9 J K^{-1} mol^{-1}, Equation 3 in Scheme 8) correlate well with the experimentally determined activation parameters ($\Delta^{\ddagger}H°$ = +57 ± 7 kJ mol^{-1}, $\Delta^{\ddagger}S°$ = −140 ± 20 J K^{-1} mol^{-1}, see section 2.3.1). A schematic reaction profile for these propagation steps is given in Figure 5, with Δ*G*° values for all steps calculated at 403 K (130 °C).

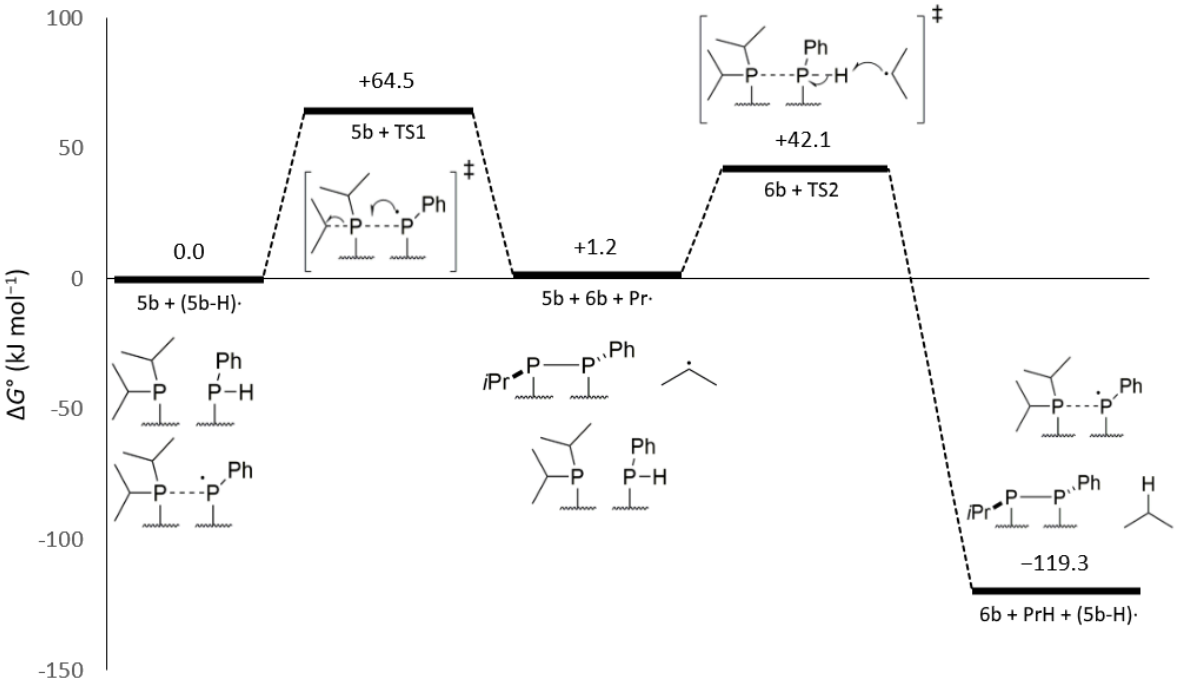

Figure 5: Schematic computed reaction profile for the propagation steps 2 and 3 shown in Scheme 8. TS1 refers to the transition state for radical (**5b**-H)· undergoing P–C bond cleavage to form Pr· and **6b**. TS2 refers to the transition state for Pr· abstracting hydrogen from **5b**. All Δ*G*° values are computed at 403 K, and given relative to the initial state.

Identification of the initiation step is, however, more complex. We believe that unimolecular dissociation of **5b** by homolytic cleavage of the weakest bond (P–*i*Pr) is not a plausible initiation step. Not only is the reaction highly energetically unfavourable (Scheme 9, Reaction 1), but it was not possible to construct a rate equation based on this initiation step that predicted second order behaviour (see SI, section 6.8.1). We conclude that a bimolecular initiation step, with 2 molecules of **5b** affording 2 radical species, is better able to account for the observed second order behaviour (see SI, section 6.8.2).

A charge transfer reaction, with 2 molecules of **5b** reacting to give a radical cation and a radical anion, would fulfil this requirement (Scheme 9, Reaction 2). However, this seems unlikely, as the rate of reaction was observed to decrease in a more polar solvent (benzonitrile). If charge separation were occurring, one would expect the opposite effect. Furthermore, the reaction is computed to be very thermodynamically unfavourable ($\Delta_r G°$ = +405.3 kJ mol^{-1} at 403 K).

Another option is the bimolecular elimination of a small molecule, either propane or hydrogen (Scheme 9, Reactions 3 and 4). This is more consistent with experimental observations, as no charged species are formed in either of these reactions. Elimination of propane would give rise to two different radicals ((**5b**-H)· and (**5b**-Pr)·), while elimination of hydrogen would afford two molecules of the same radical, (**5b**-H)·. Both steps are more thermodynamically favourable than simple unimolecular

decomposition of **5b**, due mainly to the formation of a strong (C–H or H–H) bond. In addition, both steps are likely to show a strong primary kinetic isotope effect, which would fit with our experimental observations. It should be noted that hydrogen has never been detected as a by-product to the reaction. However, if it is only formed in the initiation step, it is possible that its concentration was too low to be detected by NMR spectroscopy.

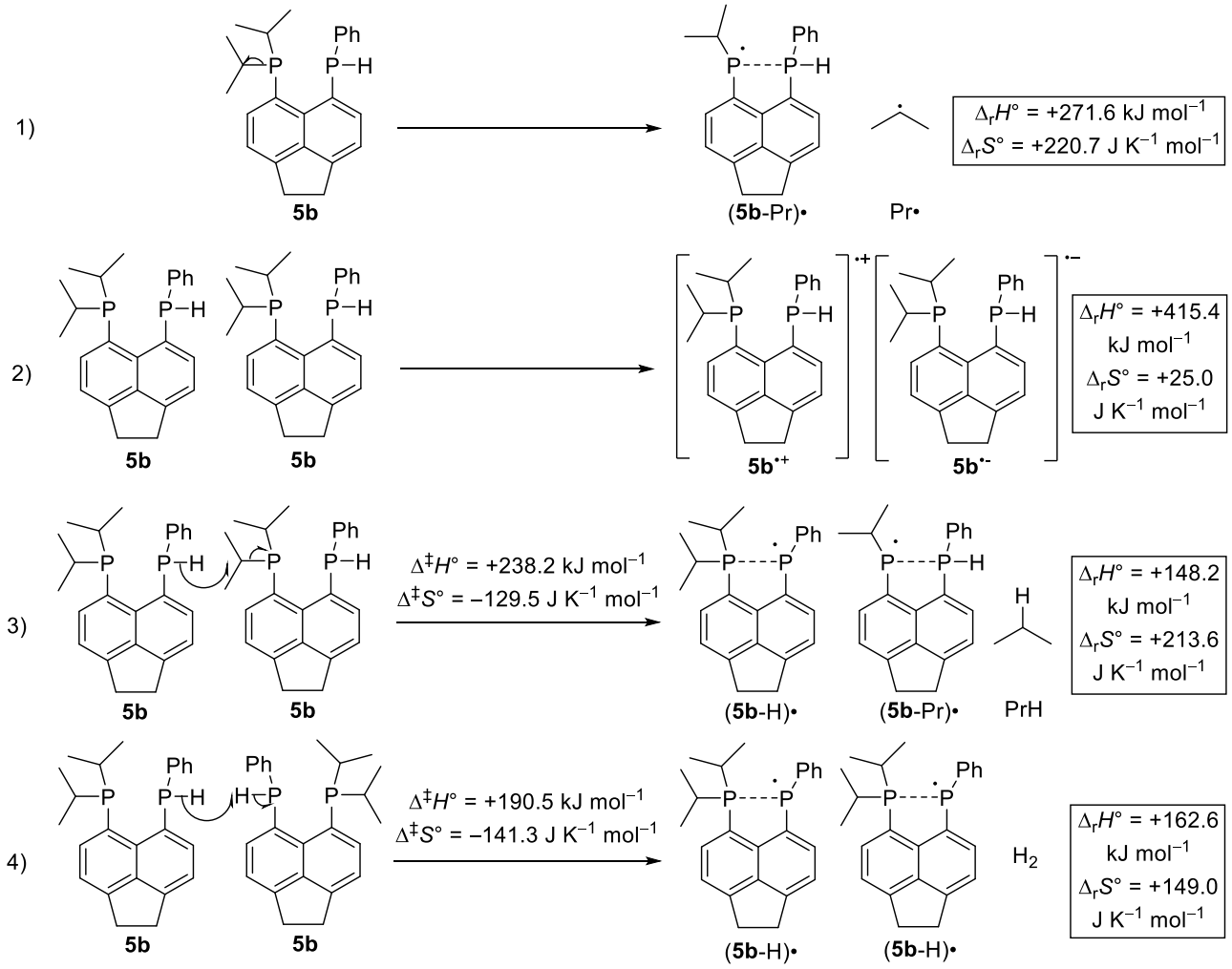

Scheme 9: Possible initiation steps for the propane elimination reaction, with computed activation parameters and thermodynamic driving forces shown. All these potential initiation steps are unlikely, because they do not fit the experimental data (1 and 2), and because they are computed to be too energetically unfavourable (all of these).

The structure of the proposed radical (**5b**-Pr)· was examined in silico, and was found to be stabilised in a similar way to (**5b**-H)· (Figure 4). Formation of the radical again results in a slight decrease in peri-distance, as well as an increase in P–P WBI (to 0.14) and significant spin delocalisation (calculated spin densities; P1 = 0.23, P9 = 0.90).[85] We thus conclude that (**5b**-Pr)· is also a plausible radical intermediate, and may be involved in the reaction.

Although these elimination reactions initially appeared plausible, location of the transition states (Figure 6) revealed them to be prohibitively high in energy. The bimolecular elimination of propane (Reaction 3, Scheme 9) has a $\Delta^‡G°$ of ca. +290 kJ mol^{-1} at 403 K, which is unlikely to be surmountable.

Bimolecular elimination of hydrogen (Reaction 4, Scheme 9) is slightly less disfavoured ($\Delta^{\ddagger}G°$ ca. +248 kJ mol^{-1} at 403 K) but this is still rather high in energy and likely to be prohibitive. It is worth noting that these computed energy barriers are subject to some uncertainty, due to the complex electronic nature of the transition states (see SI, section 7.2). It is unlikely, however, that the error associated with these calculations would reduce the computed barrier substantially.

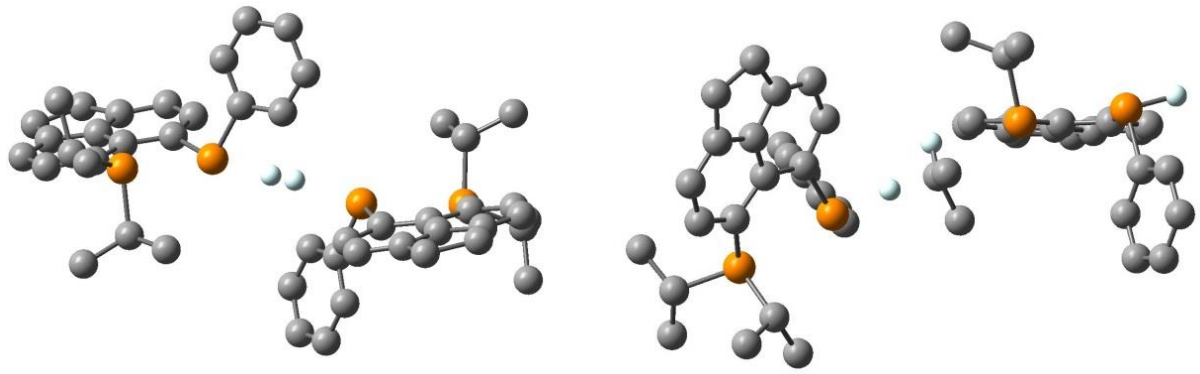

Figure 6: Located initiation transition states for bimolecular elimination of hydrogen (left) and propane (right) from **5b**.

At this stage, no other initiation steps have been proposed, and it is not clear how this reaction initiates in the absence of AIBN. This problem is of considerable interest, as the spontaneous formation of radicals from P–H and P–C functionalities is highly unusual. If the mechanism of this could be understood, it may help with the future design of similar radical transformations. Several related compounds and reactions are currently under investigation, and it is hoped that this will help shed more light on this process.

Several possible termination steps have been identified. These are discussed in more detail in the SI, section 6.7.

3 – Conclusions

By exploiting the steric strain and enforced proximity conferred by peri-substitution, a set of thermally initiated main group coupling reactions have been discovered. These reactions appear quite unique in the context of the literature, both in the "dealkanative" nature of the coupling, and the apparent involvement of radical intermediates. They are remarkably clean, diastereoselective, and occur under relatively mild conditions. In at least one case, the reaction can be facilitated by the addition of trace amounts of a radical initiator, which enhances the rate and lowers the required temperature. While the exact mechanism of radical formation (in the absence of an initiator) remains unclear, a plausible series of propagation steps have been proposed, which are supported by DFT calculations and consistent with experimental observations. The unusual geometry of the coupling precursors is likely the key to these reactions being kinetically accessible; it reduces the conformational entropy of the reacting groups, destabilises the starting material relative to the product through strain, and stabilises the proposed radical

intermediates of the reaction. We expect that this reactivity could find more general applications, although this will require a more thorough understanding of the reaction, its mechanism, and its limitations. We are particularly interested in the small molecule evolved during the coupling reaction (propane, in this case). The elimination of a C–H coupled product suggests that other couplings may be possible, and future work will focus on synthetically valuable coupling targets (i.e. C-heteroatom coupling), as well as the use of heavier main-group elements.

4 – Associated Content

Supporting Information: All synthetic procedures, experimental details, spectral characterisation, additional crystallographic information, kinetic procedures and data, and computational details can be found in the supporting information. This material is available free of charge at ACS Publications website at DOI: 10.1021/jacs.7b08682.

5 – Author Information

Corresponding Author: pk7@st-andrews.ac.uk

Notes: the authors declare no competing financial interest

6 – Acknowledgements

This work was financially supported by the EPSRC and COST action CM1302 SIPs. The authors would like to thank the EPSRC National Mass Spectrometry Facility (NMSF) and Mrs Caroline Horsburgh for running the MS spectra; and Stephen Boyer at London Metropolitan University for elemental analysis. Additionally, Laurence Taylor would like to thank Dr Tomas Lebl and Dr Filippo Stella for their help and advice on quantitative $^{31}P\{^{1}H\}$ NMR spectroscopy, determining T1 relaxation times, and simulating second order spin systems. Thanks are also due to Dr Bela Bode, for attempting high temperature EPR measurements on this reaction.

7 – Dedication

This work is dedicated to Professor Evamarie Hey-Hawkins on occasion of her recent significant birthday.

8 – Notes and References

(1) Greenberg, S.; Stephan, D. W. *Chem. Soc. Rev.* **2008**, *37* (8), 1482.
(2) Waterman, R. *Curr. Org. Chem.* **2008**, *12* (15), 1322.
(3) Leitao, E. M.; Jurca, T.; Manners, I. *Nat. Chem.* **2013**, *5* (10), 817.
(4) Nakamura, I.; Yamamoto, Y. *Chem. Rev.* **2004**, *104* (5), 2127.
(5) Jana, R.; Pathak, T. P.; Sigman, M. S. *Chem. Rev.* **2011**, *111* (3), 1417.

(6) Heravi, M. M.; Hashemi, E. *Monatsh. Chem.* **2012**, *143* (6), 861.
(7) Moore, W.; Hysell, D.; Hall, L.; Campbell, K.; Stara, J. *Environ. Heal. Persp.* **1975**, *10*, 63.
(8) Kruszynka, H.; Kruszynka, R.; Hurst, J.; Smith, R. P. *J. Toxicol. Environ. Heal.* **1980**, *6* (4), 757.
(9) ICH. *Q3D Elemental Impurities Guidance for Industry*; 2014.
(10) Power, P. P. *Nature* **2010**, *463* (7278), 171.
(11) Reichl, K. D.; Dunn, N. L.; Fastuca, N. J.; Radosevich, A. T. *J. Am. Chem. Soc.* **2015**, *137* (16), 5292.
(12) Zhao, W.; Yan, P. K.; Radosevich, A. T. *J. Am. Chem. Soc.* **2015**, *137* (2), 616.
(13) McCarthy, S. M.; Lin, Y. C.; Devarajan, D.; Chang, J. W.; Yennawar, H. P.; Rioux, R. M.; Ess, D. H.; Radosevich, A. T. *J. Am. Chem. Soc.* **2014**, *136* (12), 4640.
(14) Dunn, N. L.; Ha, M.; Radosevich, A. T. *J. Am. Chem. Soc.* **2012**, *134* (28), 11330.
(15) Zhao, W.; McCarthy, S. M.; Lai, T. Y.; Yennawar, H. P.; Radosevich, A. T. *J. Am. Chem. Soc.* **2014**, *136* (50), 17634.
(16) Whittell, G. R.; Balmond, E. I.; Robertson, A. P. M.; Patra, S. K.; Haddow, M. F.; Manners, I. *Eur. J. Inorg. Chem.* **2010**, No. 25, 3967.
(17) Spielmann, J.; Jansen, G.; Bandmann, H.; Harder, S. *Angew. Chem. Int. Ed.* **2008**, *47* (33), 6290.
(18) McPartlin, M.; Melen, R. L.; Naseri, V.; Wright, D. S. *Chem. Eur. J.* **2010**, *16* (29), 8854.
(19) Molitor, S.; Becker, J.; Gessner, V. H. *J. Am. Chem. Soc.* **2014**, *136* (44), 15517.
(20) Miller, A. J. M.; Bercaw, J. E. *Chem. Commun.* **2010**, *46* (10), 1709.
(21) Less, R. J.; Melen, R. L.; Naseri, V.; Wright, D. S. *Chem. Commun.* **2009**, No. 33, 4929.
(22) Less, R. J.; Melen, R. L.; Wright, D. S. *RSC Adv.* **2012**, *2* (6), 2191.
(23) Johnson, H. C.; Hooper, T. N.; Weller, A. S. *Top. Organomet. Chem.* **2015**, *49*, 153.
(24) Spielmann, J.; Bolte, M.; Harder, S. *Chem. Commun.* **2009**, 6934.
(25) Liptrot, D. J.; Hill, M. S.; Mahon, M. F.; MacDougall, D. J. *Chem. Eur. J.* **2010**, *16* (28), 8508.
(26) Cowley, H. J.; Holt, M. S.; Melen, R. L.; Rawson, J. M.; Wright, D. S. *Chem. Commun.* **2011**, *47* (9), 2682.
(27) Hansmann, M. M.; Melen, R. L.; Wright, D. S. *Chem. Sci.* **2011**, *2* (8), 1554.
(28) Hill, M. S.; Hodgson, M.; Liptrot, D. J.; Mahon, M. F. *Dalton Trans.* **2011**, *40*, 7783.
(29) Bellham, P.; Hill, M. S.; Kociok-Köhn, G.; Liptrot, D. J. *Chem. Commun.* **2013**, *49*, 1960.
(30) Less, R. J.; Simmonds, H. R.; Dane, S. B.; Wright, D. S. *Dalton Trans.* **2013**, *42*, 6337.
(31) Appelt, C.; Slootweg, J. C.; Lammertsma, K.; Uhl, W. *Angew. Chem. Int. Ed.* **2013**, *52* (15), 4256.
(32) Erickson, K. A.; Dixon, L. S. H.; Wright, D. S.; Waterman, R. *Inorganica Chim. Acta* **2014**, *422*, 141.
(33) Metters, O. J.; Flynn, S. R.; Dowds, C. K.; Sparkes, H. A.; Manners, I.; Wass, D. F. *ACS Catal.* **2016**, *6* (10), 6601.
(34) Hill, M. S.; Liptrot, D. J.; Macdougall, D. J.; Mahon, M. F.; Robinson, T. P. *Chem. Sci.* **2013**, *4*, 4212.
(35) Dunne, J. F.; Neal, S. R.; Engelkemier, J.; Ellern, A.; Sadow, A. D. *J. Am. Chem. Soc.* **2011**, *133*, 16782.
(36) Buch, F.; Harder, S. *Organometallics* **2007**, *26*, 5132.
(37) Greb, L.; Tamke, S.; Paradies, J. *Chem. Commun.* **2014**, *50*, 2318.
(38) Harrison, D. J.; Edwards, D. R.; McDonald, R.; Rosenberg, L. *Dalton Trans.* **2008**, 3401.
(39) Pérez, M.; Caputo, C. B.; Dobrovetsky, R.; Stephan, D. W. *Proc. Natl. Acad. Sci. U. S. A.* **2014**, *111* (30), 10917.
(40) Cella, J.; Rubinsztajn, S. *Macromolecules* **2008**, *41*, 6965.
(41) Blackwell, J. M.; Foster, K. L.; Beck, V. H.; Piers, W. E. *J. Org. Chem.* **1999**, *64*, 4887.
(42) Melen, R. L. *Chem. Soc. Rev.* **2016**, *45* (4), 775.
(43) Kilian, P.; Knight, F. R.; Woollins, J. D. *Chem. Eur. J.* **2011**, *17*, 2302.
(44) Surgenor, B. A.; Bühl, M.; Slawin, A. M. Z.; Woollins, J. D.; Kilian, P. *Angew. Chem. Int. Ed.* **2012**, *51*, 10150.
(45) Chalmers, B. A.; Bühl, M.; Arachchige, K. S. A.; Slawin, A. M. Z.; Kilian, P. *J. Am. Chem. Soc.* **2014**, *136* (17), 6247.

(46) Chalmers, B. A.; Bühl, M.; Athukorala Arachchige, K. S.; Slawin, A. M. Z.; Kilian, P. *Chem. Eur. J.* **2015**, *21* (20), 7520.
(47) Rosenthal, A. J.; Devillard, M.; Miqueu, K.; Bouhadir, G.; Bourissou, D. *Angew. Chem. Int. Ed.* **2015**, *54* (32), 9198.
(48) Zhang, S.; Wang, X.; Sui, Y.; Wang, X. *J. Am. Chem. Soc.* **2014**, *136* (42), 14666.
(49) Zhang, S.; Wang, X.; Su, Y.; Qiu, Y.; Zhang, Z.; Wang, X. *Nat. Commun.* **2014**, *5* (4127).
(50) Holthausen, M. H.; Hiranandani, R. R.; Stephan, D. W. *Chem. Sci.* **2015**, *6* (3), 2016.
(51) Holthausen, M. H.; Bayne, J. M.; Mallov, I.; Dobrovetsky, R.; Stephan, D. W. *J. Am. Chem. Soc.* **2015**, *137* (23), 7298.
(52) Devillard, M.; Brousses, R.; Miqueu, K.; Bouhadir, G.; Bourissou, D. *Angew. Chem. Int. Ed.* **2015**, *54* (19), 5722.
(53) For a quantitative evaluation of strain in some representative peri-substituted systems, see DFT calculations in: Somisara, D. M. U. K.; Bühl, M.; Lebl, T.; Richardson, N. V; Slawin, A. M. Z.; Woollins, J. D.; Kilian, P. *Chem. Eur. J.* **2011**, *17*, 2666.
(54) Taylor, L. J.; Surgenor, B. A.; Wawrzyniak, P.; Ray, M. J.; Cordes, D. B.; Slawin, A. M. Z.; Kilian, P. *Dalton Trans.* **2016**, *45*, 1976.
(55) For an example of spontaneous N–B dehydrocoupling, see: Helten, H.; Robertson, A. P. M.; Staubitz, A.; Vance, J. R.; Haddow, M. F.; Manners, I. *Chem. Eur. J.* **2012**, *18* (15), 4665.
(56) For a recent example of transition metal catalysed P–B dehydrocoupling, see: Pandey, S.; Lönnecke, P.; Hey-Hawkins, E. *Inorg. Chem.* **2014**, *53*, 8242.
(57) Reiter, S. A.; Nogai, S. D.; Karaghiosoff, K.; Schmidbaur, H. *J. Am. Chem. Soc.* **2004**, *126* (48), 15833.
(58) Kilian, P.; Philp, D.; Slawin, A. M. Z.; Woollins, J. D. *Eur. J. Inorg. Chem.* **2003**, 249.
(59) Compound 2 displays an $[ABCDX]_2$ second order spin system and, as such, gives rise to complex ^{1}H and ^{31}P NMR spectra. All relevant coupling constants have been obtained via spin simulation. Details of this can be found in section 5 of the supporting information (SI).
(60) Masuda, J. D.; Hoskin, A. J.; Graham, T. W.; Beddie, C.; Fermin, M. C.; Etkin, N.; Stephan, D. W. *Chem. Eur. J.* **2006**, *12* (34), 8696.
(61) Ghebreab, M. B.; Shalumova, T.; Tanski, J. M.; Waterman, R. *Polyhedron* **2010**, *29* (1), 42.
(62) Ray, M. J.; Slawin, A. M. Z.; Bühl, M.; Kilian, P. *Organometallics* **2013**, *32*, 3481.
(63) Compound **5b**, when previously synthesised, was obtained as an impure oil. The synthesis has been improved to give **5b** as a yellow crystalline solid, and a crystal structure of this compound has also been obtained. The crystal structure is shown in Figure 4, with data in Table 1. The improved synthesis is reported in the SI, section 4.2.
(64) Allred, A. L. *J. Inorg. Nucl. Chem.* **1961**, *17*, 215.
(65) Quin, L. D. *A Guide to Organophosphorus Chemistry*, 1st ed.; Wiley-Interscience, 2000.
(66) Stringfellow, G. B. *Organometallic Vapor-Phase Epitaxy: Theory and Practice*, 2nd ed.; Academic Press, 1998.
(67) Cowley, A. H.; Jones, R. A. *Angew. Chem. Int. Ed. Engl.* **1989**, *28* (9), 1208.
(68) Reichl, J. A.; Popoff, C. M.; Gallagher, L. A.; Remsen, E. E.; Berry, D. H. *J. Am. Chem. Soc.* **1996**, *118* (39), 9430.
(69) Katz, S. M.; Reichl, J. A.; Berry, D. H. *J. Am. Chem. Soc.* **1998**, *120* (38), 9844.
(70) Liptrot, D. J.; Arrowsmith, M.; Colebatch, A. L.; Hadlington, T. J.; Hill, M. S.; Kociok-Köhn, G.; Mahon, M. F. *Angew. Chem. Int. Ed.* **2015**, *54* (50), 15280.
(71) The arsenic analogue of the bis(phosphine) **5a**, compound **3**, was already shown to eliminate H_2 to give the arsanylidene-σ^4-phosphorane **4** (Scheme 5, top). It was hoped that replacement of one arsenic-bound hydrogen with a Ph group would preclude H_2 elimination.
(72) The novel compounds **7** and **8** are rather interesting, but they are not the focus of this paper. As such, a discussion of these compounds (including their solid state structures) is given in the section

3.2 of the SI.
(73) Thomas, I. R.; Bruno, I. J.; Cole, J. C.; Macrae, C. F.; Pidcock, E.; Wood, P. A. *J. Appl. Cryst.* **2010**, *43* (2), 362.
(74) Rate constant and error determined by three independent readings at this temperature. Error bars set to 3σ.
(75) Anslyn, E. V; Dougherty, D. A. *Modern Physical Organic Chemistry*; University Science Books, 2006.
(76) Zhang, Y.-H.; Mao, X.-A. *Phosphorus Sulfur Silicon Relat. Elem.* **2002**, *177* (10), 2409.
(77) Propane-2-*d* was identified by comparison with an authentic sample, which was prepared from the reaction of isopropyl magnesium bromide and D_2O. See section 6.6 of the SI for further details.
(78) Barton, D. H. R.; Glover, S. A.; Ley, S. V. *J. Chem. Soc., Chem. Commun.* **1977**, 266.
(79) Glover, S. A. *J. Chem. Soc., Perkin Trans. 1* **1980**, 1338.
(80) Hawari, J. A.; Engel, P. S.; Griller, D. *Int. J. Chem. Kinet.* **1985**, *17*, 1215.
(81) Under these conditions, approximately 75% of the starting material is consumed after 1 hour in the absence of 1,4-cyclohexadiene.
(82) Thermodynamic driving forces were calculated at the M06-2X/6-311+G**(PCM,benzene)//B3LYP/6-31G*(*) level. All computed thermodynamic parameters are for reagents in the standard state in the gas phase. Values are computed at 298 K, unless otherwise stated.
(83) For this comparison to hold, the rate of **6b** reacting with Pr· to reform (**5b**-H)· must be negligible, compared to the forward reaction of Pr· with **5b**. Given the significantly lower activation barrier ($\Delta^{\ddagger}G°$) for the subsequent reaction (reaction 3 in Scheme 8), this seems a reasonable assumption.
(84) Stevens, M. P. *Polymer Chemistry: An Introduction*, 3rd ed.; Oxford University Press, 1999.
(85) P···P distances are B3LYP optimised, spin density calculated at the M06-2X level. For atom labelling see Figure 4.